Chapter 2
Carbon Nanomaterials: Synthesis, Properties and Applications

Kyriakos Porfyrakis and Jamie H. Warner

2.1 Introduction

It is widely acknowledged that nanosciences and nanotechnologies are going to play an important role in our society and that they have the potential to create benefits in many technological areas including materials science, information technology as well as energy and the environment. The word "nano" is of Greek origin and means dwarf. The name reveals that we are dealing with materials and processing at fundamental length scales. Conventionally, nanotechnology involves processes and materials at length scales between 100 nm and 1 nm or below (1 nanometer is equal to 10^{-9} m).

Carbon nanomaterials are remarkable materials at the lower end of this scale. The fullerene C_{60} (or Buckyball) is 0.7 nm across, while single-walled carbon nanotubes (SWNTs) have typically diameters between 1 and 2 nm. To put this into perspective, the Earth, a football and a C_{60} molecule all have approximately spherical shape. However the Earth is about one hundred million times larger than a football, which in turn is about one hundred million times larger than C_{60}. It is really astonishing that we are able to manipulate and visualise molecules with nearly atomic precision. In this chapter we shall take a closer look at the properties and technological potential of carbon nanomaterials such as fullerenes, carbon nanotubes and graphene.

K. Porfyrakis (✉) · J.H. Warner
Department of Materials, University of Oxford, Parks Road, Oxford, OX1 3PH, UK
e-mail: kyriakos.porfyrakis@materials.ox.ac.uk; jamie.warner@materials.ox.ac.uk

S. Logothetidis (ed.), *Nanostructured Materials and Their Applications*,
NanoScience and Technology, DOI 10.1007/978-3-642-22227-6_2,

2.2 Fullerenes and Their Derivatives

The story of fullerenes as chemical structures started in the imagination of the insightful chemist E. Osawa [1] in 1970. Fifteen years later Kroto, Heath, OBrien, Curl and Smalley published their seminal paper on the discovery of C_{60} [2]. That work caused worldwide sensation and led to the award of Nobel Prize in chemistry. Initially fullerenes were produced in tiny quantities, which prevented their in-depth study. The synthetic breakthrough came in 1990. Krätschmer, Lamb, Fostiropoulos and Huffman were the first to produce macroscopic quantities of C_{60} by resistive heating of graphite rods under a He atmosphere [3]. This breakthrough led to an explosion of scientific research. Fullerenes became available in sufficient amounts for spectroscopic analysis and further chemistry. The most characteristic spectroscopic analysis comes from the ^{13}C-NMR spectrum. Figure 2.1 shows the spectrum of C_{60} in a $CS_2/CDCl_3$ mixture. Due to the curvature of the molecule, C_{60} has got the character and behaviour of a polyalkene with 60 equivalent carbon atoms of sp^2 hybridisation. Hence only one peak appears in the NMR spectrum at $\approx$143 ppm chemical shift.

C_{70} on the other hand has an elongated "rugby-ball" shape with D_{5h} symmetry. The ^{13}C-NMR spectrum of C_{70} is shown in Fig. 2.2.

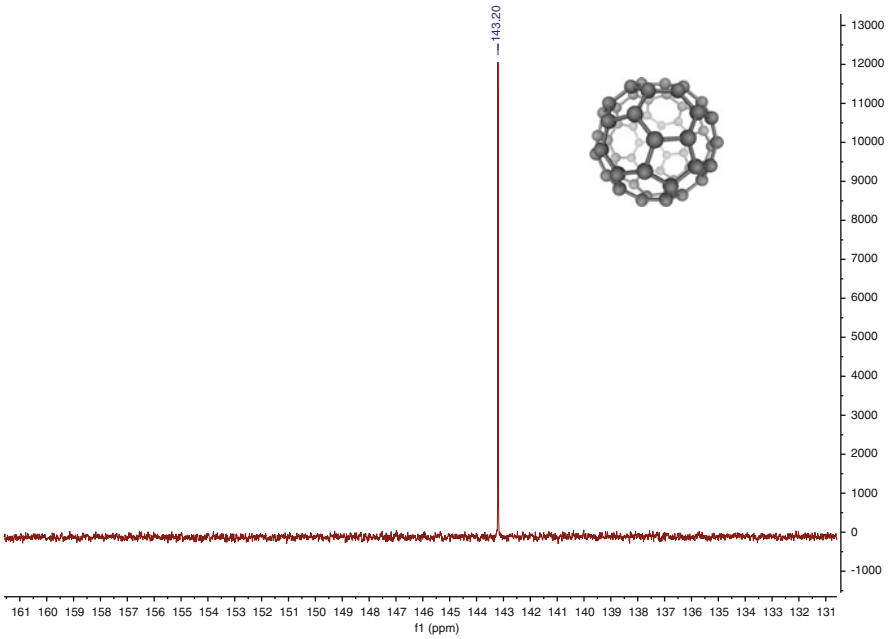

Fig. 2.1 ^{13}C-NMR spectrum of C_{60} in a $CS_2/CDCl_3$ mixture. The molecule has got icosahedral symmetry I_h. The inset shows a model of the C_{60} molecule

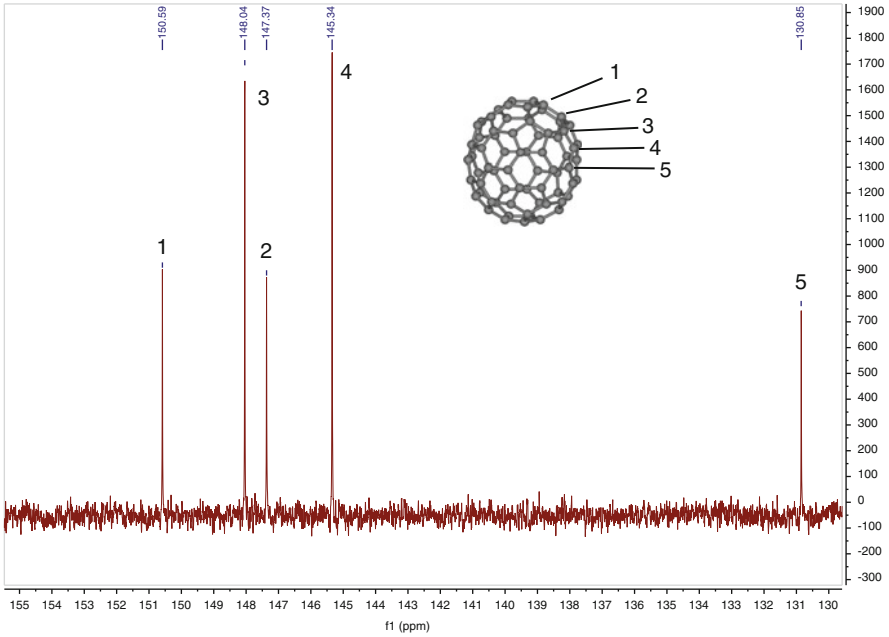

Fig. 2.2 ^{13}C-NMR spectrum of C_{70} in a $CS_2/CDCl_3$ mixture. The molecule has got D_{5h} symmetry. The inset shows a model of the C_{70} molecule

It can be seen that there are five peaks at 150.6, 148, 147.4, 145.3 and 131 ppm chemical shift. These shifts correspond to the five types of carbon atoms present at the molecule (from pole to equator), as shown in the inset. The intensity ratio of these peaks 1:2:1:2:1 corresponds to the relevant abundancy of the carbon atoms. In addition to NMR, a lot of information on the electronic structure and physicochemical properties of fullerenes has been obtained by other spectroscopies such as UV-Vis, FTIR and Raman. The more interested reader can find out more about these techniques and their application to fullerene science in the relevant bibliography and references therein [4].

2.2.1 Synthesis of Endohedral Fullerenes

Undoubtedly the most important feature of fullerene molecules is their cage-like structure. These are molecules with an enclosed interior space. It was not for long that chemists started trapping atoms inside the fullerene empty "shell". Fullerenes containing atoms or clusters in their interior are called *endohedral* fullerenes. The first endohedral metallofullerenes were lanthanum containing fullerene cages, produced by vaporisation of lanthanum-doped graphite rods. The most stable lanthanofullerene was found to be La@C_{82}. Other group-3 metals (Sc, Y) and

lanthanides (Ce, Gd, Pr, Nd, Ho, etc.) have since been encapsulated, mainly in C_{82} and C_{80}. In addition, group-2 metals (Ca, Sr, Ba) have been found to form endohedral metallofullerenes [5]. To date several elements have been encapsulated in fullerenes, including group-15 elements (N,P), noble gases (He, Ne, Ar, Kr and Xe) and molecules such as H_2 and other clusters.

2.2.2 Endohedral Metallofullerenes

Endohedral metallofullerenes are now routinely produced by the arc-discharge method. In all cases there is a charge transfer from the metal to the cage, resulting in considerable modification of the electronic properties of the cage. Figure 2.3 shows a typical arc-discharge apparatus for endohedral metallofullerene synthesis.

During operation, two doped graphite rods are brought in very close proximity and direct current (100–300 A) is passed through them forming an arc between the rods, while the helium pressure inside the arc chamber is maintained at 40–100 mbar. After a few hours of operation the rods are consumed. The remnants of the vaporised rods (slug) contain carbon nanotubes and other graphitic structures. Transmission electron microscopy (TEM) characterisation of the produced soot shows that it too is comprised mainly from amorphous carbon and graphitic structures. More importantly, the soot contains typically 10–20% fullerenes. The yield of fullerenes via the arc-discharge method is very sensitive to parameters such as He pressure, current and rod size. One discerning feature of the arc discharge shown in Fig. 2.3 is the ability to collect *and* dissolve the produced soot in an organic solvent, such as toluene and carbon disulphide, in anaerobic conditions to avoid unnecessary degradation of the endohedral metallofullerenes. The fullerenes are separated from the insolubles by soxhlet extraction. The fullerene extract is filtered, re-dissolved in fresh solvent and then passed through a high performance liquid chromatography (HPLC) apparatus in order to separate the individual fullerene species.

A particular class of endohedral metallofullerenes that has witnessed a blossoming interest over the past few years are the so-called TNTs (trimetallic nitride templated) or cluster fullerenes. They were first reported by Stevenson et al. in 1999 [6]. They were synthesised by introducing a small amount of nitrogen into the arc-discharge reactor. Although they were incorrectly identified as "small bandgap" materials initially, they were found to be very stable and quite abundant in the reactor. They can be produced with yields of 5% or higher and with a small number of isomers. Since then a large family of these materials has been synthesised with the structure $M_3N = C_{2n}$ ($34 \leq n \leq 44$) where M is a metal atom or a combination of up to three different metal atoms [7]. Some of them were even found to break the isolated pentagon rule (IPR), which normally dictates the stability of fullerene molecules [8]. $Er_3N = C_{80}$ exhibits photoluminescence from Er^{3+} ions at 1.5 μm, a wavelength region attractive for telecommunications [9]. This property gives it technological value. Comprehensive reviews on these materials can be found elsewhere [10, 11].

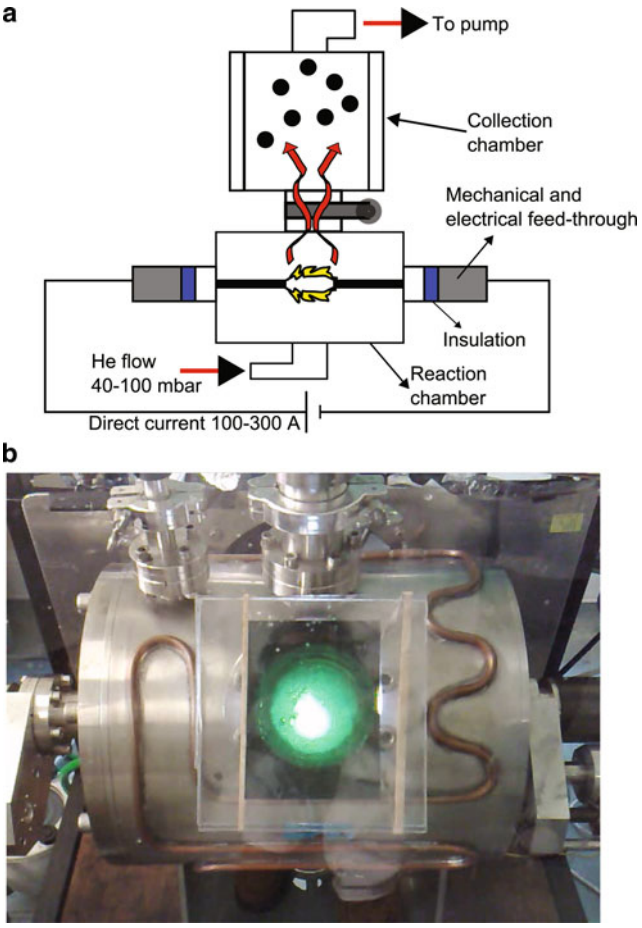

Fig. 2.3 (**a**) Schematic illustration of an arc-reactor for the production of endohedral metallofullerenes. Two doped graphite rods are brought in close proximity and high current is passed through them. An electric arc forms and the rods begin to evaporate. The soot that is produced is carried by helium to the collection chamber where the soot condenses on the liquid nitrogen-cooled walls. (**b**) Picture of the arc-discharge apparatus during operation

2.2.3 Endohedral Nitrogen Fullerenes

In addition to metallofullerenes, non-metals such as nitrogen and phosphorus have also been encapsulated in fullerenes. In contrast to metallofullerenes, these atoms appear to be more stable in smaller cages such as C_{60} and C_{70}. $N@C_{60}$ and $N@C_{70}$ are produced using the ion implantation method developed by Weidinger and co-workers at the Hahn-Meitner Institut in Germany [12]. Approximately 1 or 2 g of C_{60} are put into an effusion cell inside a vacuum chamber evacuated at a pressure of 10^{-6} mbar or lower. The effusion cell is heated at around 500°C. Under

these conditions the C_{60} is sublimed inside the chamber and begins to condense onto a water-cooled (or liquid nitrogen-cooled) copper target placed above the effusion cell. At the same time the copper target is bombarded with low energy nitrogen ions produced by an ion source. Best results are achieved using a mass-separating source, for example one producing N+ preferentially to N_2+. Typical values for the beam energy and beam current are 40 eV and 1–3 mA, respectively. The orientation of the target is such that it is located at 45° angle to both the effusion cell and the nitrogen ion source. After a few hours of operation, the copper target is covered with a fullerene layer, several tens of micrometers thick. The copper target is subsequently immersed into an organic solvent such as CS_2 in order to extract the fullerenes. The fullerene solution is ultrasonicated for a few minutes and filtered. Between 60 and 70% of $N@C_{60}/C_{60}$ mixture is dissolved in CS_2, while the rest remains insoluble. The insoluble soot comprises polymerised fullerenes and destroyed fullerene cages. The filtered solution is examined by EPR (electron paramagnetic resonance) spectroscopy. The ratio of $N@C_{60}/C_{60}$ is 10^{-4} to 10^{-5}.

The same group developed an alternative method of producing $N@C_{60}$: the glow discharge method [13]. This is a rather simpler experimental set-up compared to the ion implantation device. A quartz tube is equipped with two water-cooled copper electrodes at opposite ends. The chamber is filled with low pressure (approximately 0.1 mbar) nitrogen gas. High voltage (of the order of 1 kV) is applied across the electrodes resulting in ionisation of the nitrogen gas. At the same time, several tens of grams of C_{60} are put inside the quartz tube. The whole apparatus is then inserted in a tube oven and the system is heated up to 500°C. C_{60} sublimes and is exposed to the ionised nitrogen gas before condensing on the copper electrodes. At the end of the operation the copper electrodes are immersed in organic solvents and the produced $N@C_{60}/C_{60}$ mixture is extracted. The yield of the glow discharge method is 10^{-5} to 10^{-6} in terms of the $N@C_{60}/C_{60}$ ratio.

More recently $N@C_{60}$ has been produced using an electron cyclotron resonance (ECR) plasma source with a yield approaching 3×10^{-4} under optimised conditions [14]. However it was not clear whether this method can be used for scaled-up production of $N@C_{60}$ or even if the amounts produced are comparable with the two more established methods described earlier.

2.2.4 Molecular Synthesis of Endohedral Fullerenes

The most impressive synthetic work on endohedral fullerene synthesis stems from the group of Komatsu and Murata at Kyoto University in Japan. They developed the "molecular surgery" approach, in which the fullerene cage is opened, then doped with an atom or molecule and finally closed using a series of organic chemistry reactions [15, 16]. They created a 13-membered circular ring orifice on the cage with a sulphur atom on its rim. Then they managed to insert molecular hydrogen through the orifice into the cage with a 100% yield. Finally they used a series of reductive coupling and annealing steps in order to close the orifice and hence

produce $H_2 = C_{60}$. This is a challenging but an elegant method that may be extended in other types of endohedral fullerenes as well. Certainly $D_2 = C_{60}$ and $HD_2 = C_{60}$ seem possible as do other small atoms or molecules that can be inserted in fullerene cages in this way.

2.2.5 Purification of Endohedral Fullerenes

In nearly all cases, the synthesis of endohedral fullerenes is only the first step towards acquiring high purity individual species. Multi-stage HPLC is the established method for fullerene isolation. This is usually the most crucial and laborious step in the whole process. A combination of state-of-the-art chromatography columns tailored for fullerene purification is required for the complete isolation of isomerically pure fullerenes. Fullerenes tend to elute with size, thus C_{60} is the first one to elute followed by C_{70} and the larger cage fullerenes, including endohedral fullerenes. When fullerenes are synthesised by the arc discharge process, C_{60} accounts for about 60% of the total fullerene production whereas C_{70} represents approximately 25% of the production. The remainder 15% comprises larger empty cages as well as endohedral fullerenes. Three or four stages of HPLC through a suite of reverse-phase columns is usually enough to isolate a few milligram of high purity endohedral species [17–19]. This process may sound complicated. However it is routine compared to the purification of $N@C_{60}$ and related species. The two main obstacles are, first, the very low yields of the $N@C_{60}$ production methods and, second, the fact that C_{60} and $N@C_{60}$ are chemically almost identical. Nevertheless two groups managed independently to completely isolate $N@C_{60}$ and $N@C_{70}$ with a purity of higher than 99.5% via a combination of mutliple injections and recycling HPLC through an appropriate column (such as the Cosmosil 5-PBB by Nacalai Tesque) [20–22].

2.2.6 Properties and Applications

It comes as no surprise that the presence of incarcerated atom(s) changes the physico-chemical and electronic properties of the cage. These molecules have been found to have unusual properties such as paramagnetism [23], luminescence [24] and non-linear optical response [25]. Endohedral metallofullerenes containing gadolinium ions have been proposed for use as MRI contrast agents [26]. Their magnetic relaxivity values are higher than the relaxivities of clinically used Gd(III) chelates; hence Gd metallofullerene compounds can serve as good relaxation agents for water protons. In vivo studies of holmium-containing metallofullerenes have demonstrated their potential as radiotracers for biomedical applications [27]. Recently it has been shown that water-soluble derivatives of endohedral fullerenes can inhibit the growth of malignant tumors in vivo [28]. The mechanism of such effect is not quite clear but the authors speculate that this behaviour relates with the capacity of endohedral fullerenes to “scavenge” reactive oxygen species.

Apart from biomedical applications, another area where fullerenes in general have shown tremendous potential is optoelectronics. Empty cage fullerenes have already been used successfully in organic photovoltaic devices with an efficiency reaching 5% in polymer bulk-heterojunction devices [29]. Endohedral metallofullerenes have higher electron affinity ($\approx$3 eV) and lower ionisation potential ($\approx$7 eV) than empty cages; hence they are better electron acceptors and better electron donors. The first published work on using endohedral fullerene derivatives as electron acceptors in solar cell devices appeared very recently [30]. Ross et al. produced devices with power conversion efficiency $\geq$4%. This is quite encouraging and it looks likely that endohedral fullerenes will play a prominent role in photovoltaic cells in the near future. An additional advantage is that one can tune the HOMO-LUMO gap and the electronic properties of endohedral fullerenes by selective encapsulation of specific metal ion(s) combinations. For example $Sc = C_{82}$ has ionisation potential of 6.45 eV while $La = C_{82}$ has ionisation potential of 6.19 eV.

2.2.6.1 Endohedral Fullerenes for Quantum Information Processing

One characteristic property of endohedral fullerenes is the presence of electron spin on the molecule. The electron spin (and indeed the nuclear spin too) is a quantum property; hence quantum information can be embodied in the electron/nuclear spin state. Sc-, Y- and La-metallofullerenes have unpaired electrons [5]. The unpaired electron spin resides mostly on the cage [31]. Nitrogen containing fullerenes also carry quantum information embodied in the electron spin of the unpaired electrons of the nitrogen atom. In this case the spin-density is almost entirely localised inside the carbon cage [32]. The atomic nitrogen orbitals fit "snuggly" within the fullerene and because of the curvature of the cage, interaction with the carbon orbitals is not favourable [33]. The relative isolation of the electron spin from the environment makes these systems attractive for quantum computation schemes. For successful realisation of quantum computing there must be adequate immunity to decoherence: the degrading of quantum states due to interactions with the environment. Provided the coherence time is sufficiently long compared with the gate operation time, fault-tolerant error correction schemes can be implemented to overcome decoherence [34]. To date, NMR spin systems have hosted the most complex quantum algorithms [35]. In these systems the quantum bits, or qubits, are embodied in the slowly decohering nuclear spins of the atoms of a molecule. However, owing to the fact that the thermal energy is always large compared to the nuclear Zeeman energy in NMR experiments, NMR-based quantum computers face a fundamental limitation in scalability and appear to be practically limited to around ten qubits. Since scalability is one of the preconditions of effective quantum computation [36, 37], the practical applications of NMR-based quantum computers seem limited. EPR offers the potential to use experimentally accessible fields and temperatures to approximate pure quantum states. Endohedral fullerenes are molecular materials; therefore they are all identical at the most fundamental level.

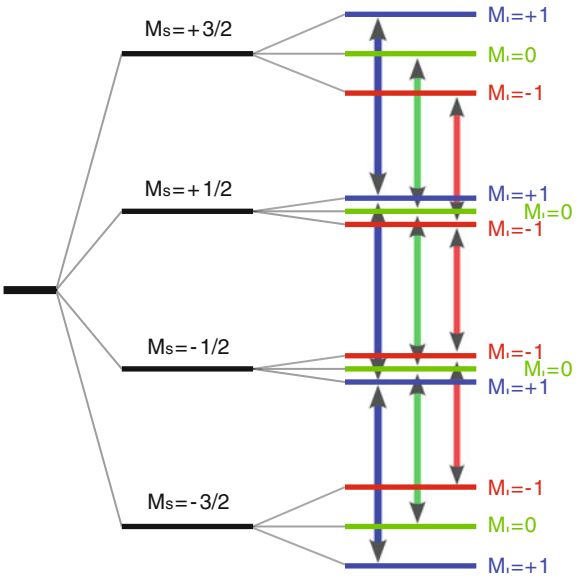

Fig. 2.4 Energy level diagram of $^{14}N@C_{60}$ in a magnetic field. $^{14}N@C_{60}$ has electron spin $S = 3/2$ and nuclear spin $I = 1$. This gives rise to a 12-level structure due to the Zeeman splitting. Taking into account just the first-order hyperfine interaction, the allowed transitions (the selection rules are $\Delta M_S = 1$ and $\Delta M_I = 0$) are triply degenerate

In addition, sophisticated chemistry can be applied to create scalable nanostructures based on these molecules.

2.2.6.2 N@C_{60} as a Spin Qubit

$N@C_{60}$ is a $S = 3/2$ electron spin system coupled to the ^{14}N nuclear spin $I = 1$ via an isotropic hyperfine interaction. This gives rise to the rich energy level diagram shown in Fig. 2.4.

Taking into account only the first-order hyperfine interaction, the nine allowed electron transitions are triply degenerate. For this reason the observed continuous-wave EPR spectrum of $N@C_{60}$ dissolved in CS_2 at room temperature (shown in Fig. 2.5) comprises three sharp resonance peaks.

The three EPR resonances are quite narrow. Their intrinsic linewidth was measured to be $\leq 0.3\,\mu$T. In fact the linewidth is mainly limited by the resolution of the spectrometer and in particular the magnet stability and field homogeneity. The ability of $N@C_{60}$ to store quantum information effectively is demonstrated by the spin-lattice relaxation time T_1 and the phase-coherence time T_2. T_2 was measured to be ≥ 0.25 ms in CS_2 solution at 160 K [38]. Pulse sequences in a typical EPR spectrometer are of the order of 30 ns. This corresponds to more than 10^4 electron spin Rabi oscillations, before decoherence occurs. These properties of the

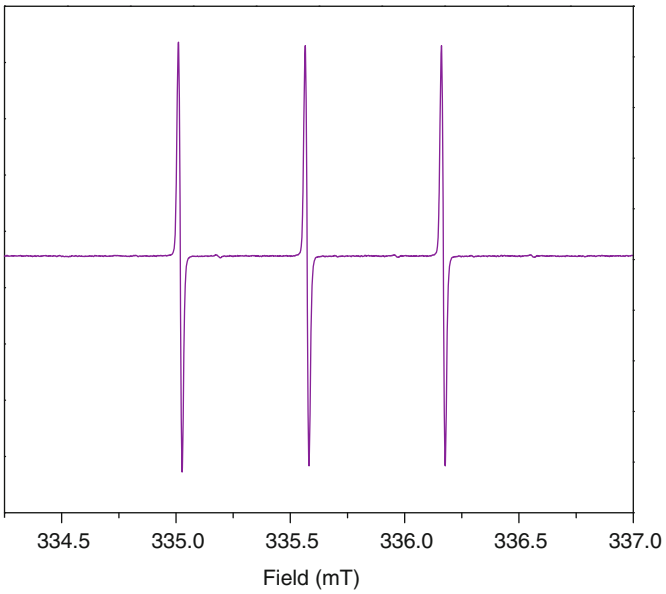

Fig. 2.5 Continuous-wave EPR spectrum of $^{14}N@C_{60}$ in a CS_2 solution. The two small resonances on either side of the central peak are associated with ^{15}N nuclei naturally abundant (less than 0.4%) in the sample

$N@C_{60}$ system ensure that it meets all the basic criteria for fault-tolerant quantum computing. Consequently $N@C_{60}$ has been proposed as a building bock of a solid-state quantum computer [39–41].

2.2.7 Chemistry of Endohedral Fullerenes

Most of the practical applications highlighted above require the construction of controlled molecular arrangements. For instance, in the case of quantum information processing, the smallest device where universal quantum gates could be applied is a two-qubit system. This requirement translates into linking two endohedral molecules together via covalent or non-covalent bonds. Moreover, dipolar coupling between adjacent spins is proportional to $1/r^3$, where r is their spatial separation. Hence, in order to control the strength of the spin-spin coupling, one must control their spatial separation. In other words, chemistry can be used to control the coupling strength of the qubits.

The chemistry of fullerenes is already well established. For example, Diels-Alder cycloaddition, Bingel, Prato and other reaction schemes have been employed in the synthesis of fullerene adducts and a rich relevant literature exists [42, 43]. The situation is markedly different when it comes to endohedral fullerenes. There are two main obstacles on the road to chemical functionalisation of endohedral

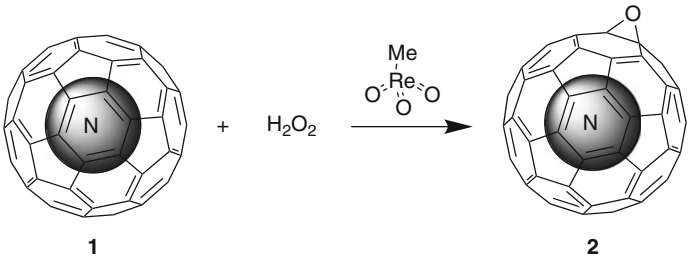

Scheme 1: The epoxidation of **1** ($N@C_{60}$) to form **2** ($N@C_{60}O$)

fullerenes. The first one is the difficulty in producing these materials in multi-milligram quantities. The second (and an equally formidable one) is the lower thermal and photolytic stability of some functionalised endohedrals such as $N@C_{60}$ adducts. The first derivative of $N@C_{60}$ was $N = C_{61}(COOEt)_2$, produced via the Bingel reaction of a $N@C_{60}/C_{60}$ mixture with diethyl bromomalonate [44]. At the time no effect on the stability of $N = C_{61}(COOEt)_2$ was reported.

It was not until a few years later that another functionalisation of $N@C_{60}$ was published. Franco et al. reported a series of fulleropyrrolidine derivatives of $N@C_{60}$ [45]. Almost simultaneously the synthesis of $N@C_{60}O$ was reported according to Scheme 1 [46].

$N@C_{60}/C_{60}$ was enriched by HPLC to 10^{-3}. The epoxide was formed by reacting **1** with H_2O_2 in the presence of MeO_3Re under ambient conditions for 12 h to give **2**. It was observed that **2** is stable in the dark at room temperature. However, dissolved in toluene and exposed to ambient light, **2** exhibited a linear decay of EPR intensity with a half life of approximately 2 days.

Since that work was published the functionalisation chemistry of $N@C_{60}$ has been expanded. We now know that most additions to the cage inflict some degree of EPR signal loss on $N@C_{60}$. This implies that either some $N@C_{60}$ is destroyed or that the nitrogen atom escapes from the fullerene cage. The limited availability of high purity $N@C_{60}$ combined with its thermal and photo-instability might initially look like an insurmountable obstacle to further chemistry. However, it is possible to tune reaction conditions in such a manner that a significant "number of spins" survive the reaction. $N@C_{60}$ was reacted with 4-nitrobenzaldehyde and *N*-methylglycine, according to the Prato reaction as shown in Scheme 2 [47].

An excess of $N@C_{60}$ was refluxed with the aldehyde and sarcosine in toluene for 2 h under nitrogen. Under these conditions **3** ($N = C_{69}H_{10}N_2O_2$) was produced with 31% yield. Crutially, the EPR signal intensity of the product mixture was found to be arround 73% of the initial $N@C_{60}$ signal.

One step further is the production of a *half-filled* endohedral fullerene dimer using again the pyrrolidine functionalisation (Scheme 3) [48].

After reflux in toluene for 2 days, the C_{60}-azo-C_{60} dimer was produced in 95% yield. In order to preserve the nitrogen spin signal, the same reaction with $N@C_{60}$ was performed for approximaely 2 h. **4** ($N = C_{60}$-azo-C_{60}) was produced

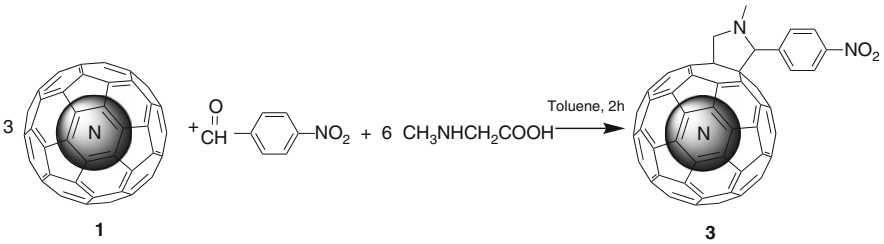

Scheme 2: Synthesis of $N = C_{69}H_{10}N_2O_2$ via the Prato reaction scheme

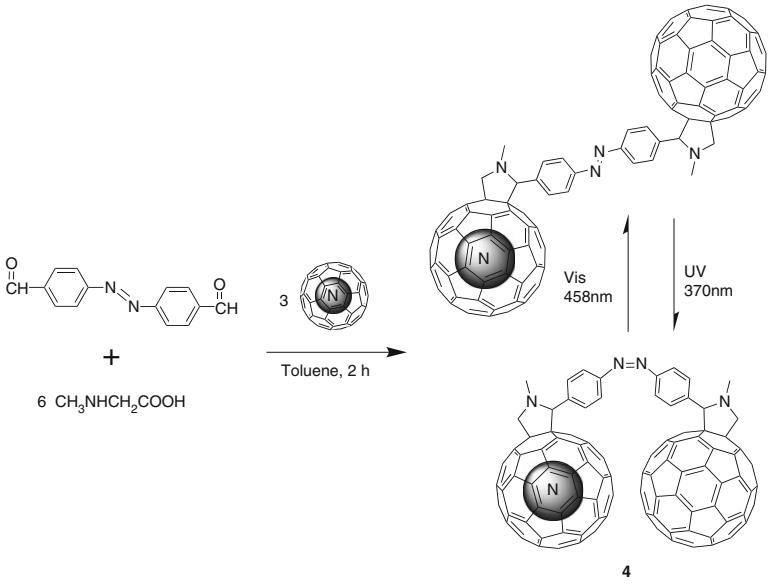

Scheme 3: Synthesis of photo-switchable dimer $N@C_{60}$-azo-C_{60} and its photoisomerisation

with 30% yield. Its EPR signal was found to be approximately 70% of the starting material. The azobenzene moiety is one of the most efficient photoisomerised molecules. Exposed to visible light it is mostly in the trans- form. Upon irradiation with UV light, it changes to the cis-isomer. We performed the same isomerisation with **4**. Using pulse EPR, molecular rotation correlation times $\tau_c = 37.2 \pm 1.6$ ps for the trans- and $\tau_c = 34.8 \pm 2.7$ ps for the cis-isomers were measured, respectively. This subtle difference is attributed to the difference in size between the two isomers. The trans is the bulkier of the two hence its tumbling is slightly slower than the cis which leads to a longer rotation correlation time.

The beauty of this scheme is that it not only retains most of the $N@C_{60}$ signal, but also affords both the dimer and the monomer products by manipulation of the reagent molar ratios. This is the first time that a two-step reaction to yield

an asymmetric endohedral fullerene dimer in a controlled way seems feasible. For example, a $^{14}N@C_{60}$-$^{15}N@C_{60}$ dimer could be possible by first doing the reaction with excess aldehyde to produce the $^{14}N@C_{60}$ monomer and then reacting the monomer with $^{15}N@C_{60}$ to produce the asymmetric dimer. Such a molecule would be the first fullerene two-qubit system. Also the bridge molecule would act s a photo-switch modulating the distance between the fullerene cages and hence the interaction between the qubits. It must be noted that even though this is a unique molecule, a directly bonded $N@C_{60}$-C_{60} dimer was synthesized previously via the high speed vibration milling technique (HSVM) method [49]. However the purity of $N@C_{60}$ was too low to allow for in-depth spectroscopic study of that molecule.

The synthetic schemes analysed in the previous paragraphs involved C_{60} or $N@C_{60}$ the chemistry of which is very similar to C_{60}. Endohedral metallofullerenes have not been used extensively in functionalisation schemes. One reason is that most of them involve C_{82} or C_{80}. These are cages with lower symmetry that give rise to a number of isomers and multi-adducts. On the other hand, metallofullerenes are thermally robust unlike $N@C_{60}$ as we have seen above. Although their chemistry is not so well developed (compared to C_{60}), they are beginning to be available in multi-milligram quantities of high purity materials. Some synthetic protocols for metallofullerene adducts have begun to appear in recent years [50–53]. As more endohedral metallofullerenes become available in larger amounts, their chemistry will be developed further, and sophisticated synthons such as an endohedral metallofullerene dimer may become attainable.

In addition to covalent bonding, non-covalent interactions present an attractive route toward the assembly of arrays of endohedral fullerenes. Such interactions include hydrogen bonding, van der Waals interactions, $\pi - \pi$ stacking interactions and coordination chemistry. Porphyrins, cyclodextrins, calixarenes and other macrocycles can be complexed with fullerenes in order to create supramolecular arrays. Although weak in comparison to covalent bonds, it is well known that very stable structures can be achieved through the cooperative effect of such interactions. An advantage of these interactions is that they are driven with an inherent ability to "self-correct" due to their thermodynamic nature [54]. It looks likely that these schemes can be extended to endohedral fullerenes too.

2.2.8 One-Dimensional, Two-Dimensional Arrays and Beyond

The structure of one-dimensional arrays of fullerenes is relatively straightforward. Fullerene molecules self-assemble into ordered arrays inside SWNTs. The process is spontaneous upon heating and the resulting structures are called nanotube "peapods" [55]. Metallofullerene peapod structures are well established [56, 57]. What is less understood are the peapod electronic structure and the effect of filling on the spin properties of the metallofullerenes. This is partly due to the fact that SWNTs come as a mixture of semi-conducting and metallic ones and with

many paramagnetic impurities that interfere with the magnetic properties of the encapsulated endohedral fullerenes. Thermally unstable molecules such as $N@C_{60}$ and its derivatives can also be inserted into SWNTs using solution methods or supercritical fluids [58, 59]. It has even been suggested that the thermal stability of $N@C_{60}$ is enhanced in the peapod structures compared to its crystalline form [60].

Two-dimensional supramolecular structures can form on surfaces by exploiting non-covalent (mainly hydrogen bonding) interactions between the constituent molecules. Some molecular networks can form porous structures that can act as hosts for fullerenes. The arrangement of the guest fullerene molecules is largely controlled by the size and shape of the network pores. Hexagonally packed C_{60} heptamers have been formed in a perylene tetra-carboxylic di-imide (PTCDI)-melamine network on a silver-terminated silicon surface [61]. Single C_{60} molecules have been incorporated in a trimesic acid (TMA) molecular network on graphite [62]. Recently, a strontium titanate ($SrTiO_3$) "waffle" surface was used as a template for arrays of paired endohedral fullerenes ($Er_3N = C_{80}$) [63]. The molecules "fit" like eggs fitting into an egg carton. This work shows that it is possible to arrange endohedral fullerenes in ordered, two-dimensional arrays in a controlled manner and should pave the way for more intricate arrangements of endohedral molecules. In principle, such patterns can be extended in to three-dimensional networks too. Such architectures are prerequisites for many technological applications including nanoelectronics and quantum information processing.

2.3 Graphene

Graphene is a two-dimensional sheet of carbon atoms arranged in a hexagonal structure with sp^2 bonding, shown in Fig. 2.6. Layers of graphene are stacked on top of each other in an AB orientation to form the well- known three-dimensional solid graphite. The layers of graphene are not directly bonded to each but instead are held together within graphite by van der Waals forces. This enables the exfoliation of graphite to form single graphene layers. Two layers of graphene are known as bilayer graphenes, whist 3–6 layers are known as few layer graphenes (Fig. 2.7). Rich physics has been observed in graphene layers [64], along with superior mechanical properties [65]. This has stimulated a buzz in the international community about the possible future exploitation of graphene in electronics and mechanical strengthening applications.

2.3.1 Synthesis

Graphenewas first discovered in 2004 by the Geim group at the University of Manchester [66]. This was the major breakthrough that stimulated an entirely new field. Their process was to mechanically exfoliate graphite by repeatedly

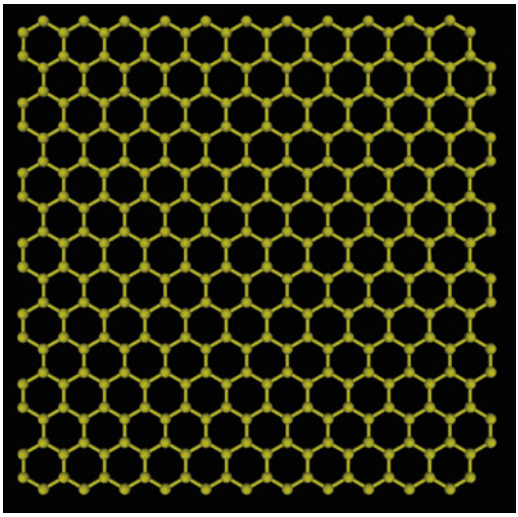

Fig. 2.6 Graphene sheet with arm-chair edge termination at the sides and zigzag termination at top and bottom edges

removing layers of high quality graphite (such as highly orientated pyrolytic graphite (HOPG)) using scotch tape. This reduced the average number of layers in the graphite flakes, which were then stamped onto a silicon substrate coated with a thin 300 nm layer of SiO_2. This process produced only a small number of graphene layers with respect to thicker multi-layered graphite pieces on the surface of the silicon substrate and thus finding graphene was like looking for a needle in a haystack. The key innovation by the Geim group was to use optical microscopy to visually inspect the graphene layers and use a change in the optical contrast that arises from an interference effect caused by the presence of the SiO_2 layer. Optical microscopy enabled thin graphene monolayers to be identified by their weak contrast and then checked with atomic force microscopy to determine the height. Andre Geim and Konstantin Novoselov were awarded the Nobel Prize in Physics 2010 for their groundbreaking experiments with graphene.

While the scotch tape exfoliation method sparked the graphene boom, it is widely acknowledged that this approach has severe limitations in the commercial uptake of graphene in the electronics industry due to the relatively small size of the graphene layers that are produced. Solution phase chemical exfoliation is another technique that has successfully been used to obtain graphene and few layer graphene [67]. In this approach, graphene layers are peeled apart from one another by the combination of ultrasound sonication in a suitable polar solvent or aqueous surfactant system. This leads to flakes of graphene, bilayer graphene and few layer graphene mixed among large chunks of graphite. The large pieces of graphite are removed from the solution by centrifuging at low speeds. Most success in solution phase exfoliation has been achieved using solvents like *N*-methyl-2-pyrrolidone (NMP), Dimethylformamide (DMF), 1,2-dichloroethane and aqueous surfactant systems such as sodium dodecyl sulphate (SDS) and sodium cholate. It seems that currently the chemical exfoliation methods do not produce large area flakes of

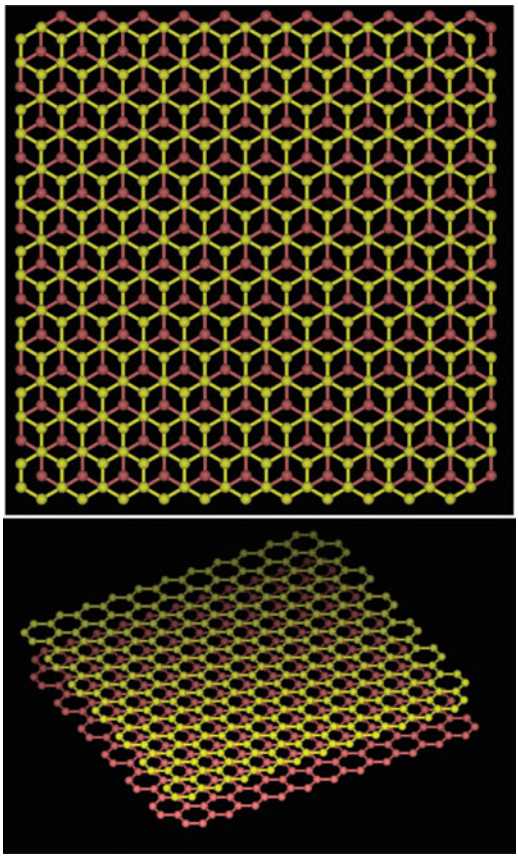

Fig. 2.7 Bilayer graphene with AB stacking. Top layer is *yellow* and bottom layer is *pink*

graphene needed for electronic applications, but can produce macroscopic amounts. The most promising routes for growing large area graphene layers are the surface precipitation growth on SiC substrate [68], and the epitaxial growth on catalytic metals such as nickel [69] and copper [70] using chemical vapour deposition. Graphene grown on these substrates can be transferred to other substrates such as quartz using a variety of techniques [71–73]. The major challenge remaining in this approach is to get the charge carrier mobility up to those reported for the mechanical exfoliation technique.

2.3.2 Properties and Applications

Graphene has raised massive interest in the international electronics community by exhibiting ambi-polar electric field effect behaviour at high carrier concentrations of up to 10^{13} cm^{-2} and charge carrier mobilities exceeding 15,000 $cm^2V^{-1}s^{-1}$.

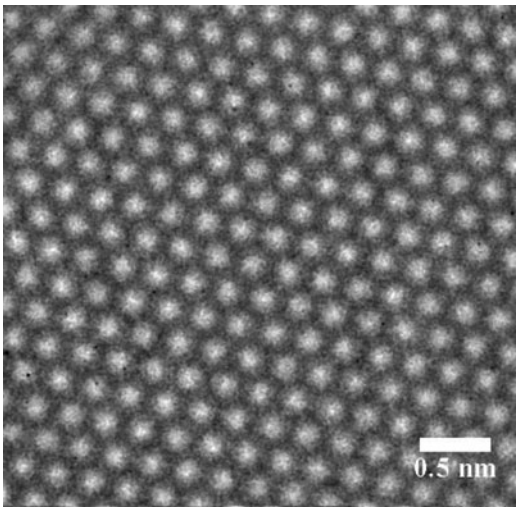

Fig. 2.8 Aberration corrected high-resolution transmission electron microscopy image of graphene taken at an accelerating voltage of 80 kV

Graphene exhibits ballistic charge transport on the sub-micrometer scale [74] and also quantum Hall effects at room temperature [75]. The charge carriers move so fast in graphene that they are best described by the Dirac equation for relativistic particles than the Schrödinger equation. Graphene has immense potential in nanoelectronic applications and for this to be realised, large area mm^2 sheets of high quality graphene or bilayer graphene are needed.

Graphene also boasts one of the highest mechanical strengths ever reported [65]. This makes it very appealing for blending with polymers for reinforcement. Since graphene is only one atomic layer thick and mechanically stable it is ideal for using as an ultrathin transparent support for high resolution electron microscopy [76]. Figure 2.8 shows a high-resolution transmission electron microscopy image of graphene showing the atomic structure.

This image was taken with aberration correction to achieve sub-Angstrom spatial resolution and at a low accelerating voltage of 80 kV in order to minimise damage [77]. The periodic atomic structure is easily removed by post-processing digital filtering leaving images of nanoparticles or molecules as if they were suspended in free space.

2.4 Carbon Nanotubes

A SWNT can be formed by rolling up a graphene sheet to form a tubular structure. The properties of carbon nanotubes are defined by their chirality, which is linked to the way they are rolled up into a cylinder. A chiral vector C_h is used to classify the chirality of a nanotube in terms of (n,m) values, where $C_h = na_1 + ma_2$ as shown in Fig. 2.9. A translational vector T, perpendicular to C, defines the length of the

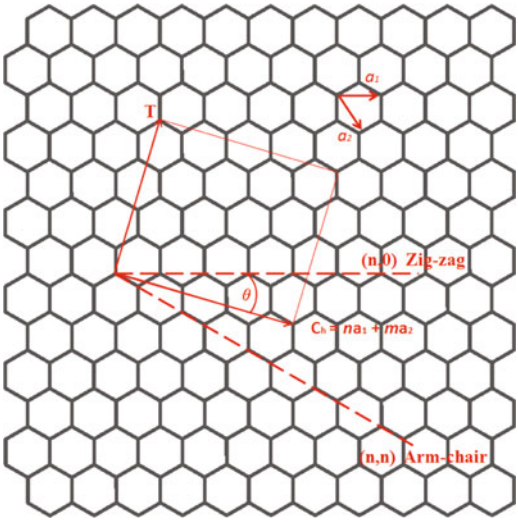

Fig. 2.9 Determining chirality of single-walled carbon nanotubes

nanotubes' unit cell. The chiral angle θ defines the direction of C relative to the basis vector a_1. The (n,m) values of a nanotube indicate whether it will be semiconducting or metallic. When n-m is divisible by three the nanotubes are typically metallic, alternatively they are semiconducting. Arm-chair SWNTs are defined as $n = m$, i.e., (n,n), zigzag as (n,0), and chiral when $n \neq m$.

As the radius of a nanotubes decreases, the degree of curvature increases. This places significant strain on the sp^2 carbon bonds and leads to an increase in the chemical reactivity of smaller diameter nanotubes and a reduced stability [78], [79]. For semiconducting carbon nanotubes, the bandgap generally increases for decreasing nanotubes radius. This leads to diameter-dependent photoluminescence from SWNTs [80]. Multi-walled carbon nanotubes are formed by concentric addition of larger tubes around a core inner SWNT. Inter-wall coupling leads to MWNTs being primarily metallic. Figure 2.10 shows an end-on perspective view of a (18,0) SWNT.

2.4.1 Synthesis

Observations of nanotubes were reported as far back as 1952 by L. V. Radushkevich and V. M. Lukyanovich in the Soviet *Journal of Physical Chemistry* [81]. However, it is widely acknowledged that the spark that ignited the field of carbon nanotubes was the seminal paper by Sumio Iijima in 1991 [82]. His combination of observation and interpretation was critical in developing nanotube science. The use of transmission electron microscopy was crucial to this discovery. Advances in electron microscopy now enable the atomic structure of nanotubes to be directly imaged, such as in Fig. 2.11 [79].

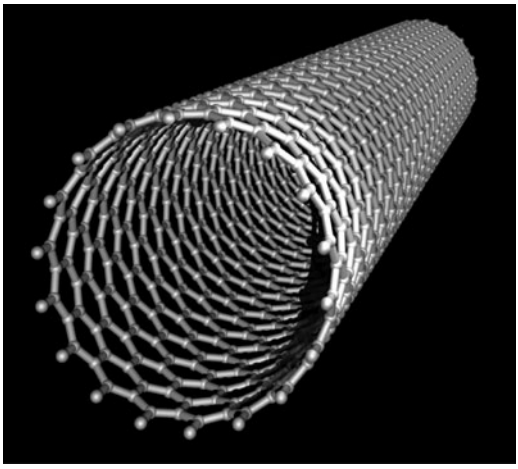

Fig. 2.10 An end-on perspective view of a (18,0) SWNT

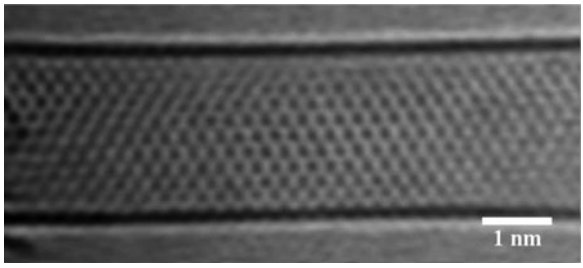

Fig. 2.11 Aberration-corrected high-resolution transmission electron microscopy image of a single-walled carbon nanotube showing the atomic structure

Several techniques have been developed to produce carbon nanotubes in large scale quantities. These are arc-discharge [83], laser ablation [84, 85], chemical vapour deposition [86] and high pressure carbon monoxide (HiPCO). Each of these techniques has its own merits depending on what applications the nanotubes are to be used for. Arc-discharge tends to produce large quantities, but often contains a significant amount of catalyst nanoparticles that are usually magnetic and amorphous carbon. Arc-discharge is a desirable route to fabricating nanotubes with diameters between 1.2 and 1.6 nm. Laser ablation tends to produce a higher yield of nanotubes compared to catalysts and amorphous carbon, but does not have the ability to produce the same volume of material that arc-discharge can. HiPCO nanotubes are generally smaller in diameter than arc-discharge or laser ablation with diameters between 0.7 and 1.2 nm. CVD-grown nanotubes often lack the structural quality of nanotubes produced via laser ablation or arc-discharge, but are ideal for growing vertical forests or nanotubes on substrates for nanoelectronics. The diameter distribution of CVD-grown nanotubes is often broader than other methods.

Purification of carbon nanotubes is one of the most challenging aspects of their research. It is important to remove catalyst particles and amorphous carbon to obtain pristine nanotubes. Amorphous carbon is generally removed by either burning in air below the nanotubes decomposition temperature or refluxing in H_2O_2. Catalysts

are generally Ni, Co or Fe and can be removed by refluxing in acids such as HCl and HNO_3. Both of these methods also damage the nanotubes and reduce the total amount of product. Alternative way to remove catalyst particles is to use high speed centrifugation methods or to anneal at high temperatures (1,200°C) under high dynamic vacuum. Density gradient ultracentrifugation has recently been demonstrated as a technique to separate metallic and semiconducting nanotubes from each other [87].

2.4.2 Applications

Carbon nanotubes are promising for a wide range of applications involving electronics, mechanical strengthening, photonics and heat dissipation. Semiconducting SWNTs emit photoluminescence in the NIR wavelength region between 1.1 and 2.0 μm, which makes them appealing as biological chromophores and in telecommunications applications. Metallic nanotubes have low resitivity and a high capacity to carry larger currents than metals. The electronic transport of nanotubes shows quantised transport down to the single electron level. Significant advances have been made in developing field effect transistors comprising semiconducting nanotubes operating at GHz frequencies. Young's modulus measurements of nanotubes are on the order of TPa and the incorporation into polymers leads to light-weight ultrastrong composites that are already commercially available. Carbon nanotubes have excellent thermal conductivity up to 2,000 W/m/K, which makes them appealing for heat dissipation. Because of these properties, carbon nanotubes have been hailed as the "wonder material" for the twenty-first century.

2.5 Summary

In this chapter we focused on carbon nanomaterials. We described their synthesis and we analysed their electronic and physico-chemical properties with practical applications in mind. Perhaps the most exotic application is the use of these molecules as building blocks for a quantum device. Quantum phenomena are inherent in atoms and molecules and carbon nanomaterials are the perfect playground to study quantum phenomena even at room temperature. We discussed the synthetic developments in endohedral fullerene chemistry. We focused particularly on various chemical syntheses that have been applied to give endohedral fullerene adducts: from monomers and small fullerene dimers to larger one-dimensional and two-dimensional array architectures.

We discussed the properties of graphene and carbon nanotubes. We showed that quantum phenomena can be studied using these materials and innovative science can be performed at the nanoscale. The unique properties of these materials put them at the forefront of many technologies.

There is little doubt that there are advantages but also complications with carbon nanomaterials and with their potential in applications ranging from medicine to quantum information. It was our intention to highlight the properties that make these molecules unique and the main challenges that need to be overcome. Two Nobel Prizes have been awarded so far for discoveries related to fullerenes and graphene. This is testament of the importance of carbon nanomaterials. Research to date has demonstrated that fullerenes, graphene, carbon nanotubes and their derivatives are not far from finding their way in the market place via established nanotechnological applications.

References

1. E. Osawa, Kagaku (Kyoto) **25**, 854 (1970)
2. H. Kroto, J. Heath, S. O'Brien, R. Curl, R. Smalley, Nature **318**(6042), 162 (1985)
3. W. Kratschmer, L. Lamb, K. Fostiropoulos, D. Huffman, Nature **347**(6291), 354 (1990)
4. K. Kadish, R. Ruoff, *Fullerenes: Chemistry, Physics and Technology* (Wiley, New York, USA, 2000)
5. H. Shinohara, Rep. Prog. Phys. **63**(6), 843 (2000)
6. S. Stevenson, G. Rice, T. Glass, K. Harich, F. Cromer, M. Jordan, J. Craft, E. Hadju, R. Bible, M. Olmstead, K. Maitra, A. Fisher, A. Balch, H. Dorn, Nature **401**(6748), 55 (1999)
7. S. Yang, L. Dunsch, J. Phys. Chem. B **109**(25), 12320 (2005)
8. S. Yang, M. Kalbac, A. Popov, L. Dunsch, Chem. – A Eur. J. **12**(30), 7856 (2006). DOI 10.1002/chem.200600261
9. R. Macfarlane, D. Bethune, S. Stevenson, H. Dorn, Chem. Phys. Lett. **343**(3-4), 29 (2001)
10. S. Stevenson, P. Fowler, T. Heine, J. Duchamp, G. Rice, T. Glass, K. Harich, E. Hajdu, R. Bible, H. Dorn, Nature **408**(6811), 427 (2000)
11. L. Dunsch, S. Yang, Small **3**(8), 1298 (2007). DOI 10.1002/smll.200700036
12. T. Murphy, T. Pawlik, A. Weidinger, M. Hohne, R. Alcala, J. Spaeth, Phys. Rev. Lett. **77**(6), 1075 (1996)
13. A. Weidinger, M. Waiblinger, B. Pietzak, T. Murphy, Appl. Phys. A – Mater. Sci. Process. **66**(3), 287 (1998)
14. T. Kaneko, S. Abe, H. Ishida, R. Hatakeyama, Phys. Plasmas **14**(11) (2007). DOI 10.1063/1.2814049
15. K. Komatsu, M. Murata, Y. Murata, Science **307**(5707), 238 (2005). DOI 10.1126/science.1106185
16. Y. Murata, M. Murata, K. Komatsu, J. Am. Chem. Soc. **125**(24), 7152 (2003). DOI 10.1021/ja0354162
17. H. Okimoto, R. Kitaura, T. Nakamura, Y. Ito, Y. Kitamura, T. Akachi, D. Ogawa, N. Imazu, Y. Kato, Y. Asada, T. Sugai, H. Osawa, T. Matsushita, T. Muro, H. Shinohara, J. Phys. Chem. C **112**(15), 6103 (2008). DOI 10.1021/jp711776j
18. T. Akasaka, S. Okubo, M. Kondo, Y. Maeda, T. Wakahara, T. Kato, T. Suzuki, K. Yamamoto, K. Kobayashi, S. Nagase, Chem. Phys. Lett. **319**(1–2), 153 (2000)
19. D. Leigh, J. Owen, S. Lee, K. Porfyrakis, A. Ardavan, T. Dennis, D. Pettifor, G. Briggs, Chem. Phys. Lett. **414**(4–6), 307 (2005). DOI 10.1016/j.cplett.2005.08.090
20. T. Suetsuna, N. Dragoe, W. Harneit, A. Weidinger, H. Shimotani, S. Ito, H. Takagi, K. Kitazawa, Chem. – A Eur. J. **8**(22), 5079 (2002)
21. P. Jakes, K. Dinse, C. Meyer, W. Harneit, A. Weidinger, Phys. Chem. Chem. Phys. **5**(19), 4080 (2003)

22. M. Kanai, K. Porfyrakis, A. Briggs, T. Dennis, Chem. Commun. (2), 210 (2004). DOI 10.1039/b310978h
23. A. Bartl, L. Dunsch, U. Kirbach, G. Seifert, Synth. Met. **86**(1–3), 2395 (1997). International Conference on the Science and Technology of Synthetic Metals, Snowbird, UT, July 28–August 02, 1996
24. M.A.G. Jones, R.A. Taylor, A. Ardavan, K. Porfyrakis, G.A.D. Briggs, Chem. Phys. Lett. **428**(4–6), 303 (2006). DOI 10.1016/j.cplett.2006.06.094
25. E. Xenogiannopoulou, S. Couris, E. Koudoumas, N. Tagmatarchis, T. Inoue, H. Shinohara, Chem. Phys. Lett. **394**(1–3), 14 (2004). DOI 10.1016/j.cplett.2004.06.093
26. R. Bolskar, A. Benedetto, L. Husebo, R. Price, E. Jackson, S. Wallace, L. Wilson, J. Alford, J. Amer. Chem. Soc. **125**(18), 5471 (2003). DOI 10.1021/ja03400984
27. D. Cagle, S. Kennel, S. Mirzadeh, J. Alford, L. Wilson, Proc. Natl. Acad. Sci. USA **96**(9), 5182 (1999)
28. J.J. Yin, F. Lao, J. Meng, P.P. Fu, Y. Zhao, G. Xing, X. Gao, B. Sun, P.C. Wang, C. Chen, X.J. Liang, Mol. Pharmacol. **74**(4), 1132 (2008). DOI 10.1124/mol.108.048348
29. W. Ma, C. Yang, X. Gong, K. Lee, A. Heeger, Adv. Funct. Mater. **15**(10), 1617 (2005). DOI 10.1002/adfm.200500211
30. R.B. Ross, C.M. Cardona, D.M. Guldi, S.G. Sankaranarayanan, M.O. Reese, N. Kopidakis, J. Peet, B. Walker, G.C. Bazan, E. Van Keuren, B.C. Holloway, M. Drees, Nat. Mater. **8**(3), 208 (2009). DOI 10.1038/NMAT2379
31. G. Morley, B. Herbert, S. Lee, K. Porfyrakis, T. Dennis, D. Nguyen-Manh, R. Scipioni, J. van Tol, A. Horsfield, A. Ardavan, D. Pettifor, J. Green, G. Briggs, Nanotechnology **16**(11), 2469 (2005). DOI 10.1088/0957-4484/16/11/001
32. B. Plakhutin, N. Breslavskaya, E. Gorelik, A. Arbuznikov, J. Mol. Struct.-Theorem **727**(1–3), 149 (2005). DOI 10.1016/j.theochem.2005.02.031
33. H. Mauser, N. Hommes, T. Clark, A. Hirsch, B. Pietzak, A. Weidinger, L. Dunsch, Angew Chem Int Ed **36**(24), 2835 (1997)
34. A. Steane, Phys. Rev. Lett. **77**(5), 793 (1996)
35. L. Vandersypen, M. Steffen, G. Breyta, C. Yannoni, M. Sherwood, I. Chuang, Nature **414**(6866), 883 (2001)
36. D. DiVincenzo, Fortschritte der physik-progress of Physics **48**(9–11), 771 (2000)
37. C. Bennett, D. DiVincenzo, Nature **404**(6775), 247 (2000)
38. J. Morton, A. Tyryshkin, A. Ardavan, K. Porfyrakis, S. Lyon, G. Briggs, J. Chem. Phys. **124**(1) (2006). DOI 10.1063/1.2147262
39. W. Harneit, Phys. Rev. A **65**(3, Part A), 032322 (2002). DOI 10.1103/PhysRevA.65
40. A. Ardavan, M. Austwick, S. Benjamin, G. Briggs, T. Dennis, A. Ferguson, D. Hasko, M. Kanai, A. Khlobystov, B. Lovett, G. Morley, R. Oliver, D. Pettifor, K. Porfyrakis, J. Reina, J. Rice, J. Smith, R. Taylor, D. Williams, C. Adelmann, H. Mariette, R. Hamers, Philos. Trans. R. Soc. Lond. Ser. A – Math. Phys. Eng. Sci. **361**(1808), 1473 (2003). DOI 10.1098/rsta.2003.1214. Discussion Meeting of the Royal-Society, London, England, March 13–14, 2002
41. S. Benjamin, A. Ardavan, G. Andrew, D. Briggs, D. Britz, D. Gunlycke, J. Jefferson, M. Jones, D. Leigh, B. Lovett, A. Khlobystov, S. Lyon, J. Morton, K. Porfyrakis, M. Sambrook, A. Tyryshkin, J. Phys. Condens. Matter **18**(21, Sp. Iss. SI), S867 (2006). DOI 10.1088/0953-8984/18/21/S12
42. R. Taylor, *Lecture Notes on Fullerene Chemistry: A Handbook for Chemists* (Imperial College Press, London, UK, 1999)
43. A. Hirsch, M. Brettreich, F.B. Wudl, *Fullerenes: Chemistry and Reactions* (Wiley VCH, Weinheim, Germany, 2004)
44. B. Pietzak, M. Waiblinger, T. Murphy, A. Weidinger, M. Hohne, E. Dietel, A. Hirsch, Chem. Phys. Lett. **279**(5–6), 259 (1997)
45. L. Franco, S. Ceola, C. Corvaja, S. Bolzonella, W. Harneit, M. Maggini, Chem. Phys. Lett. **422**(1–3), 100 (2006). DOI 10.1016/j.cplett.2006.02.046
46. M. Jones, D. Britz, J. Morton, A. Khlobystov, K. Porfyrakis, A. Ardavan, G. Briggs, Phys. Chem. Chem. Phys. **8**(17), 2083 (2006). DOI 10.1039/b601171c

47. J. Zhang, J.J.L. Morton, M.R. Sambrook, K. Porfyrakis, A. Ardavan, G.A.D. Briggs, Chem. Phys. Lett. **432**(4–6), 523 (2006). DOI 10.1016/j.cplett.2006.10.116
48. J. Zhang, K. Porfyrakis, J.J.L. Morton, M.R. Sambrook, J. Harmer, L. Xiao, A. Ardavan, G.A.D. Briggs, J. Phys. Chem. C **112**(8), 2802 (2008). DOI 10.1021/jp711861z
49. B. Goedde, M. Waiblinger, P. Jakes, N. Weiden, K. Dinse, A. Weidinger, Chem. Phys. Lett. **334**(1–3), 12 (2001)
50. T. Wakahara, Y. Iiduka, O. Ikenaga, T. Nakahodo, A. Sakuraba, T. Tsuchiya, Y. Maeda, M. Kako, T. Akasaka, K. Yoza, E. Horn, N. Mizorogi, S. Nagase, J. Amer. Chem. Soc. **128**(30), 9919 (2006). DOI 10.1021/ja062233h
51. O. Lukoyanova, C.M. Cardona, J. Rivera, L.Z. Lugo-Morales, C.J. Chancellor, M.M. Olmstead, A. Rodriguez-Fortea, J.M. Poblet, A.L. Balch, L. Echegoyen, J. Amer. Chem. Soc. **129**(34), 10423 (2007). DOI 10.1021/ja071733n
52. Y. Takano, A. Yomogida, H. Nikawa, M. Yamada, T. Wakahara, T. Tsuchiya, M.O. Ishitsuka, Y. Maeda, T. Akasaka, T. Kato, Z. Slanina, N. Mizorogi, S. Nagase, J. Amer. Chem. Soc. **130**(48), 16224 (2008). DOI 10.1021/ja802748q
53. T. Akasaka, T. Kono, Y. Takematsu, H. Nikawa, T. Nakahodo, T. Wakahara, M.O. Ishitsuka, T. Tsuchiya, Y. Maeda, M.T.H. Liu, K. Yoza, T. Kato, K. Yamamoto, N. Mizorogi, Z. Slanina, S. Nagase, J. Amer. Chem. Soc. **130**(39), 12840+ (2008). DOI 10.1021/ja802156n
54. J. Lindsey, New J. Chem. **15**(2–3), 153 (1991)
55. B. Smith, M. Monthioux, D. Luzzi, Nature **396**(6709), 323 (1998)
56. K. Hirahara, K. Suenaga, S. Bandow, H. Kato, T. Okazaki, H. Shinohara, S. Iijima, Phys. Rev. Lett. **85**(25), 5384 (2000)
57. J.H. Warner, A.A.R. Watt, L. Ge, K. Porfyrakis, T. Akachi, H. Okimoto, Y. Ito, A. Ardavan, B. Montanari, J.H. Jefferson, N.M. Harrison, H. Shinohara, G.A.D. Briggs, Nano Lett. **8**(4), 1005 (2008). DOI 10.1021/nl0726104
58. F. Simon, H. Kuzmany, H. Rauf, T. Pichler, J. Bernardi, H. Peterlik, L. Korecz, F. Fulop, A. Janossy, Chem. Phys. Lett. **383**(3–4), 362 (2004). DOI 10.1016/j.cplett.2003.11.039
59. A. Khlobystov, D. Britz, J. Wang, S. O'Neil, M. Poliakoff, G. Briggs, J. Mater. Chem. **14**(19), 2852 (2004). DOI 10.1039/b404167d
60. S. Toth, D. Quintavalle, B. Nafradi, L. Korecz, L. Forro, F. Simon, Phys. Rev. B **77**(21) (2008). DOI 10.1103/PhysRevB.77.214409
61. J. Theobald, N. Oxtoby, M. Phillips, N. Champness, P. Beton, Nature **424**(6952), 1029 (2003). DOI 10.1038/nature01915
62. S. Griessl, M. Lackinger, F. Jamitzky, T. Markert, M. Hietschold, W. Heckl, J. Phys. Chem. B **108**(31), 11556 (2004). DOI 10.1021/jp049521p
63. D.S. Deak, F. Silly, K. Porfyrakis, M.R. Castell, J. Amer. Chem. Soc. **128**(43), 13976 (2006). DOI 10.1021/ja0634369
64. A.K. Geim, K.S. Novoselov, Nat. Mater. **6**(3), 183 (2007)
65. C. Lee, X. Wei, J.W. Kysar, J. Hone, Science **321**(5887), 385 (2008). DOI 10.1126/science.1157996
66. K. Novoselov, A. Geim, S. Morozov, D. Jiang, Y. Zhang, S. Dubonos, I. Grigorieva, A. Firsov, Science **306**(5696), 666 (2004)
67. Y. Hernandez, V. Nicolosi, M. Lotya, F.M. Blighe, Z. Sun, S. De, I.T. McGovern, B. Holland, M. Byrne, Y.K. Gun'ko, J.J. Boland, P. Niraj, G. Duesberg, S. Krishnamurthy, R. Goodhue, J. Hutchison, V. Scardaci, A.C. Ferrari, J.N. Coleman, Nat. Nanotechnol. **3**(9), 563 (2008). DOI 10.1038/nnano.2008.215
68. C. Berger, Z. Song, X. Li, X. Wu, N. Brown, C. Naud, D. Mayou, T. Li, J. Hass, A.N. Marchenkov, E.H. Conrad, P.N. First, W.A. de Heer, Science **312**(5777), 1191 (2006). DOI 10.1126/science.1125925
69. A. Reina, X. Jia, J. Ho, D. Nezich, H. Son, V. Bulovic, M.S. Dresselhaus, J. Kong, Nano Lett. **9**(1), 30 (2009). DOI 10.1021/nl801827v
70. X. Li, W. Cai, J. An, S. Kim, J. Nah, D. Yang, R. Piner, A. Velamakanni, I. Jung, E. Tutuc, S.K. Banerjee, L. Colombo, R.S. Ruoff, Science **324**(5932), 1312 (2009). DOI 10.1126/science.1171245

71. K. Novoselov, D. Jiang, F. Schedin, T. Booth, V. Khotkevich, S. Morozov, A. Geim, Proc. Nat. Acad. Sci. USA **102**(30), 10451 (2005). DOI 10.1073/pnas.0502848102
72. K. Novoselov, A. Geim, S. Morozov, D. Jiang, M. Katsnelson, I. Grigorieva, S. Dubonos, A. Firsov, Nature **438**(7065), 197 (2005). DOI 10.1038/nature04233
73. Y. Zhang, Y. Tan, H. Stormer, P. Kim, Nature **438**(7065), 201 (2005). DOI 10.1038/nature04235
74. X. Du, I. Skachko, A. Barker, E.Y. Andrei, Nat. Nanotechnol. **3**(8), 491 (2008). DOI 10.1038/nnano.2008.199
75. K.S. Novoselov, Z. Jiang, Y. Zhang, S.V. Morozov, H.L. Stormer, U. Zeitler, J.C. Maan, G.S. Boebinger, P. Kim, A.K. Geim, Science **315**(5817), 1379 (2007). DOI 10.1126/science.1137201
76. J.C. Meyer, C.O. Girit, M.F. Crommie, A. Zettl, Nature **454**(7202), 319 (2008). DOI 10.1038/nature07094
77. J.H. Warner, M.H. Ruemmeli, L. Ge, T. Gemming, B. Montanari, N.M. Harrison, B. Buechner, G.A.D. Briggs, Nat. Nanotechnol. **4**(8), 500 (2009). DOI 10.1038/NNANO.2009.194
78. S. Niyogi, M. Hamon, H. Hu, B. Zhao, P. Bhowmik, R. Sen, M. Itkis, R. Haddon, Acc. Chem. Res. **35**(12), 1105 (2002). DOI 10.1021/ar010155r
79. J.H. Warner, F. Schaeffel, G. Zhong, M.H. Ruemmeli, B. Buechner, J. Robertson, G.A.D. Briggs, ACS Nano **3**(6), 1557 (2009). DOI 10.1021/nn900362a
80. M. O'Connell, S. Bachilo, C. Huffman, V. Moore, M. Strano, E. Haroz, K. Rialon, P. Boul, W. Noon, C. Kittrell, J. Ma, R. Hauge, R. Weisman, R. Smalley, Science **297**(5581), 593 (2002)
81. L. Radushkevich, V. Lukyanovich, Zurn Fisic Chim **26**, 88 (1952)
82. S. Iijima, Nature **354**(6348), 56 (1991)
83. T. Ebbesen, P. Ajayan, Nature **358**(6383), 220 (1992)
84. T. Guo, P. Nikolaev, A. Rinzler, D. Tomanek, D. Colbert, R. Smalley, J. Phys. Chem. **99**(27), 10694 (1995)
85. T. Guo, P. Nikolaev, A. Thess, D. Colbert, R. Smalley, Chem. Phys. Lett. **243**(1–2), 49 (1995)
86. M. Joseyacaman, M. Mikiyoshida, L. Rendon, J. Santiesteban, Appl. Phys. Lett. **62**(6), 657 (1993)
87. M.S. Arnold, A.A. Green, J.F. Hulvat, S.I. Stupp, M.C. Hersam, Nat. Nanotechnol. **1**(1), 60 (2006). DOI 10.1038/nnano.2006.52